GC-MS, HPLC, UV-VIS, AND FTIR CHARACTERIZATION OF BIOACTIVE PHYTOCONSTITUENTS IN THE HYDRO-ETHANOLIC LEAF EXTRACT OF *DIGERA MURICATA* (L.) MART: A MULTI-ANALYTICAL APPROACH

S. TAMILARASAN[1], R. VIDYA[2,*]

[1]Research Scholar, Department of Biochemistry, School of Life Sciences, Vels Institute of Science, Technology and Advanced Studies (VISTAS), Pallavaram, Chennai, India

[2]Associate Professor & Head, Department of Biochemistry, School of Life Sciences, Vels Institute of Science, Technology and Advanced Studies (VISTAS), Pallavaram, Chennai, India

*Corresponding author: R Vidya; *Email: vidyabiochem@gmail.com

ABSTRACT

Digera muricata (L.) Mart (Amaranthaceae) has a well-documented history of therapeutic application in South Asian folk medicine, yet the identity of its constituent bioactive molecules has remained largely uncharacterised at the molecular level. Our previous study established that the hydro-ethanolic leaf extract harbours exceptional quantities of total phenolics, flavonoids, saponins, tannins, and steroids, pointing to substantial pharmacological potential. The present work follows from that quantitative baseline by applying multi-instrumental characterization techniques, viz., Gas Chromatography-Mass Spectrometry (GC-MS), High-Performance Liquid Chromatography (HPLC), Ultraviolet-Visible (UV-Vis) spectroscopy, and Fourier-Transform Infrared (FTIR) spectroscopy, to characterise the specific molecular constituents responsible for those activities. GC-MS analysis resolved 30 chromatographic peaks, with n-hexadecanoic acid (palmitic acid, 57.08%) and octadecanoic acid (10.97%) as dominant constituents, accompanied by phytol, tetradecanoic acid, and muskolactone among the biologically relevant minor components. HPLC profiling at 280 nm tentatively identified 12 polyphenolic constituents, with rutin (39.73%), ellagic acid (14.12%), and catechin (11.49%) accounting for the majority of the peak area. The UV-Vis analysis showed that the major absorptions were found at 202.6 nm and 250.1 nm, which were associated with aromatic conjugation and flavonoid Band-II chromophores. FTIR established the presence of hydroxyl, aliphatic, alkene, aromatic, and ether functionalities, which were in agreement with the GC-MS and HPLC profiles. The data collectively have offered a molecular basis of the antioxidant, anti-inflammatory, and anticancer potentials of this plant, and have identified rutin, ellagic acid, palmitic acid and phytol as priority compounds to be isolated and their bioactivity validated.

Keywords: Amaranthaceae, *Digera muricata*, FTIR, GC-MS, HPLC, Palmitic acid, Polyphenols, Phytochemistry, Rutin

How to cite this article: Tamilarasan S, Vidya R. GC-MS, HPLC, UV-VIS, And Ftir Characterization Of Bioactive Phytoconstituents In The Hydro-Ethanolic Leaf Extract Of Digera Muricata (L.) Mart: A Multi-Analytical Approach. Int J Drug Deliv Technol. 2026;16(65s):1226-1234. DOI: 10.25258/ijddt.16.65s.126

INTRODUCTION

The renewed global interest in plant-derived therapeutics over the past two decades reflects both the unsatisfied burden of chronic and infectious disease and the inherent chemical diversity that medicinal plants offer as a source of bioactive leads [1,2]. Within this context, wild edible plants belonging to the family Amaranthaceae have attracted increasing pharmacological scrutiny, given that several members, including *Amaranthus* spp., *Aerva lanata*, and *Celosia argentea*, are known to produce structurally diverse polyphenols, terpenoids, and alkaloids with demonstrable *in vitro* and *in vivo* bioactivity [3,4,5]. *Digera muricata* (L.) Mart, colloquially known as 'Cancali soppu' across peninsular India and 'jungle spinach' in parts of East Africa, is one of the lesser-studied members of this family despite centuries of documented ethnomedicinal use [6].

In the Indian Ayurvedic system, *D. muricata* preparations have been employed as a laxative, bowel astringent, diuretic, and galactagogue; root decoctions are traditionally administered to lactating women to stimulate milk production, and the aerial parts have been used in treating urinary disorders and renal inflammation [6,7]. These applications have been partially substantiated by experimental work demonstrating the plant's capacity to attenuate carbon tetrachloride-induced nephrotoxicity in rats, an effect attributed broadly to its polyphenolic content [7]. Further studies have established antiproliferative activity against prostate and cervical carcinoma cell lines [8,9], broad-spectrum antimicrobial activity including inhibition of *Klebsiella pneumoniae, Staphylococcus aureus*, and *Candida albicans* [10], antioxidant activity as demonstrated by HPTLC fingerprinting [11], and the capacity to synthesise antibacterial gold nanoparticles

[12]. Despite this accumulating pharmacological evidence, none of these studies has identified, at the molecular level, the specific phytoconstituents responsible for the observed activities.

Our preceding study addressed part of this deficit by conducting systematic qualitative and quantitative phytochemical profiling of the *D. muricata* leaf hydro-ethanolic extract, confirming the presence of tannins, saponins, flavonoids, steroids, terpenoids, alkaloids, anthraquinone, polyphenols, glycosides, coumarins, emodins, and anthocyanins [13]. Quantitative spectrophotometric assays yielded notably high values for total phenolics (246.82 mg GAE/g) and total flavonoids (193.18 mg QE/g), values that compare favourably with, those reported for other medicinally significant Amaranthaceae species such as *Amaranthus viridis* (total phenolics 209 to 330.0 mg GAE 100 g^{-1}) [14] and *Aerva javanica* (total phenolics 91.39± 5.1 mg GAE/g; total flavonoids 63.5±2.7 mg QE/g) [15]. However, the spectrophotometric methods employed in that study quantify compound classes in bulk, providing no information about the identity, relative proportions, or structural features of the individual molecules within each class. This constitutes a critical knowledge gap: high bulk phenolic content does not, in itself, predict the specific antioxidant mechanisms operative, nor does it indicate which individual compounds warrant isolation and clinical investigation.

The present study was therefore designed to bridge that gap through an integrated, multi-analytical characterisation strategy. GC-MS was selected to profile the volatile and semi-volatile fraction, which is expected to be dominated by terpenoids, fatty acids, and their derivatives, compounds that are invisible to spectrophotometric phenolic assays yet frequently account for significant proportions of the biological activity of plant extracts [16]. Reverse-phase HPLC with UV detection at 280 nm was employed to fractionate and tentatively identify the polar polyphenolic fraction, which encompasses the flavonoids and phenolic acids responsible for the majority of the radical-scavenging capacity. UV-Vis spectroscopy was used to characterise chromophoric classes through characteristic electronic transitions, and FTIR spectroscopy was applied to map the functional group architecture of the whole extract. Each technique is informative independently, but their collective application allows cross-validation of findings and yields a substantially more complete molecular portrait of the extract than any single method could provide [17].

This multi-platform approach is consistent with recent best practice in medicinal plant characterisation as evidenced by comparable studies on Amaranthaceae members and other ethnomedicinally relevant herbs. To the best of our knowledge, this is the first report combining GC-MS, HPLC, UV-Vis, and FTIR analyses for *D. muricata* leaf extract, and the findings are discussed in the context of recent literature on the pharmacological relevance of the identified compounds.

MATERIALS AND METHODS

Plant Material and Preparation of Extract

Digera muricata leaves were collected from the cultivator and authenticated by Dr. N. Mathivanan, Director and Head, Centre for Advanced Studies in Botany, University of Madras, Chennai (Voucher No. MUBL1030). The leaves were dried in shade, powdered coarsely and macerated in cold under the conditions of hydro-ethanolic solvent (ethanol:distilled water, 70:30 v/v) over 24 h with intervals of shaking. The resultant slurry was filtered through Whatman No. 1 filter paper; the filtrate was concentrated under reduced pressure and used for all downstream analyses.

GC-MS Analysis

GC-MS analysis was conducted according to Dowlath et al. [18] with slight modifications on a Shimadzu GC-MS 2010 Plus system equipped with an AOC-20i autosampler and interfaced to an electron-ionisation mass spectrometer. The chromatographic column was an RTX-5MS capillary column (30 m × 0.32 mm i.d. × 0.50 µm film thickness). Ultra-high-purity helium (99.999%) served as the carrier gas at a constant flow rate of 1.73 mL/min. Temperature was setted from 40°C (isotherm, 2 min), ramped at 8°C/min to 150°C, continued at 8°C/min to 250°C, and held isothermally at 280°C for 20 min (total run time: 51.25 min). The injection volume was 0.5 µL (split ratio 10:1); injector and ion-source temperatures were 270°C and 200°C, respectively. Mass spectra were acquired in full-scan mode at 70 eV over m/z 40–450. Compound identification was accomplished by comparison of mass spectral fragmentation patterns against the NIST 2011 and WILEY7 libraries (combined >62,000 reference spectra), with identity accepted at match scores ≥80%. All relative concentrations were expressed as normalised peak area percentages.

HPLC Analysis

Reverse-phase HPLC analysis of the phenolic and flavonoid fractions was performed using a Shimadzu Class-VP V6.14SP2 system equipped with an autosampler (20 µL fixed injection loop) and a UV-Vis variable-wavelength detector. Gradient elution was performed with mobile phase A (water:acetic acid, 25:1 v/v) and mobile phase B (methanol): solvent B was increased to 50% over 4 min and subsequently to 80% over the next 6 min, at a constant flow rate of 1.0 mL/min. Samples were run for 25 min and detection was at 280 nm (deuterium lamp). Polyphenolic compounds were tentatively identified by comparison of retention

times (RT) with those reported in the literature for equivalent reversed-phase conditions [19,20].

UV-Vis Spectroscopy

The hydro-ethanolic extract was scanned across 200–1100 nm using a Perkin Elmer Lambda series UV-Vis spectrophotometer. All measurements were performed in duplicate; the mean absorbance values are reported. Characteristic absorption maxima were assigned to chromophoric classes based on established electronic transition theory for phenolics and flavonoids.

FTIR Spectroscopy

FTIR spectra were recorded on a Perkin Elmer FTIR spectrophotometer at 400–4000 cm^{-1} in transmittance mode. The extract was deposited as a thin film on the ATR/KBr crystal and allowed to dry prior to measurement. All analyses were performed in duplicate and mean peak positions are reported. Functional group assignments were based on correlation with standard spectroscopic reference charts and established literature values for plant phenolics and lipids.

RESULTS

GC-MS Compound Identification

The hydro-ethanolic extract of *D. muricata* was analyzed by GC-MS, which separated 30 chromatographic peaks in the course of the 51.25-min run (Figure 1). Twelve peaks were selected for discussion on the basis of identified biological relevance (Table 1); the complete peak list is provided in Table 2. The chromatogram was dominated by a single major peak at RT 13.883 min, corresponding to n-hexadecanoic acid (palmitic acid, $C_{16}H_{32}O_2$, MW 256), which accounted for 57.08% of the total normalised peak area. The second abundantly available compound was octadecanoic acid (stearic acid, $C_{18}H_{36}O_2$, MW 284) at RT 15.949 min (10.97%), followed by muskolactone ($C_{15}H_{28}O_2$) at RT 15.740 min (3.66%). Phytol (diterpene alcohol, $C_{20}H_{40}O$, MW 296.5) was identified at RT 15.445 min (1.51%), and its acetate derivative was detected at RT 12.531 min (0.45%). Additional minor constituents included 1,2-benzenedicarboxylic acid diethyl ester (RT 9.942 min, 2.70%), the identity of which as a genuine plant metabolite rather than a laboratory plasticizer contaminant requires cautious interpretation; tetradecanoic acid (myristic acid, 1.16%); 1-hexadecene (1.07%); phenol (0.84%); hexadecanoic acid ethyl ester (0.59%); 6-dodecanone (0.54%); and 1-tetradecanol (0.37%).

Table 1: GC-MS identification of major bioactive compounds in the hydro-ethanolic extract of *Digera muricata* leaf

Peak	RT (min)	Compound	Biological Activity
1	7.394	1-Tetradecanol	Antibacterial
2	8.805	Phenol	Antioxidant, anti-carcinogenic, anti-inflammatory
3	9.942	1,2-Benzenedicarboxylic acid, diethyl ester	Antimicrobial, antifouling
4	11.724	Tetradecanoic acid	Antioxidant, cancer-preventing, nematicide, larvicidal
5	12.531	Phytol acetate	Anticancer, anti-inflammatory, hepatoprotective, nephroprotective
6	12.650	6-Dodecanone	Antibacterial
7	13.883	n-Hexadecanoic acid (Palmitic acid)	Antioxidant, hypocholesterolemic, 5α-reductase inhibitor
8	14.162	Hexadecanoic acid, ethyl ester	Antioxidant, hypocholesterolemic, pesticide
9	15.124	1-Hexadecene	Antimicrobial
10	15.445	Phytol	Antimicrobial, anticancer, diuretic, anti-inflammatory
11	15.949	Octadecanoic acid (Stearic acid)	Antioxidant, anti-inflammatory, LDL-lowering
12	15.740	Muskolactone	Fragrance, antimicrobial

Table 2: Identification of active compounds in hydro-ethanolic extract of *Digera muricata* using GCMS

Peak	R. Time	Area %	Height %	Molecular Formula	Molecular Weight	Name of the compounds
1	7.394	0.37	0.62	$C_{14}H_{30}O$	214	1-Tetradecanol
2	8.805	0.84	1.45	$C_{14}H_{22}O$	206	Phenol
3	9.942	2.70	2.34	$C_{12}H_{14}O_4$	222	1,2-Benzenedicarboxylic acid, diethyl ester

4	11.724	1.16	1.14	$C_{14}H_{28}O_2$	228	Tetradecanoic acid
5	12.531	0.45	0.74	$C_{22}H_{42}O_2$	338	Phytol, acetate
6	12.650	0.54	0.50	$C_{12}H_{18}O$	178	6-Dodecanone
7	12.767	0.70	0.22	$C_8H_{10}Cl_2$	192	5,5-Dichloro-6,6-dimethyl-Spirohexan-4-ONE
8	13.042	1.93	2.05	$C_{23}H_{36}O_4$	376	Phthalic acid, butyl undecyl ester
9	13.473	1.19	1.36	$C_21H_{42}O_2$	326	Eicosanoic acid, methyl ester
10	13.642	1.24	1.90	$C_{14}H_{22}N_2O$	234	Lidocaine
11	13.692	2.55	3.50	$C_{17}H_{24}O_3$	276	7,9-Di-tert-butyl-1-oxaspiro(4,5)deca-6,9-diene-2,8-dione
12	13.883	57.08	54.80	$C_{16}H_{32}O_2$	256	n-Hexadecanoic acid
13	14.162	0.59	0.97	$C_{18}H_{36}O_2$	284	Hexadecanoic acid, ethyl ester
14	14.983	0.41	0.41	$C_{10}H_{18}O_2$	170	Allyl heptanoate
15	15.124	1.07	1.24	$C_{16}H_{32}$	224	1-Hexadecene
16	15.303	0.97	0.96	$C_{24}H_{72}O_{12}SI_{12}$	888	Tetracosamethylcyclododecasiloxane
17	15.445	1.51	1.91	$C_{20}H_{40}O$	246	Phytol
18	15.518	1.61	1.72	$C_{19}H_{36}O_3$	312	Oxiraneundecanoic acid, 3-pentyl-, methyl ester, trans-
19	15.740	3.66	2.85	$C_{15}H_{28}O_2$	240	Muskolactone
20	15.800	0.97	2.01	$C_{22}H_{13}NO_4$	355	Ethyl 1-hexyl-4-hydroxy-2(1h)-oxo-3-quinolinecarboxylate
21	15.850	0.75	1.19	$C_6H_9N_3O_2$	155	2,6-Dimethoxy-4-aminopyrimidine
22	15.949	10.97	9.81	$C_{18}H_{36}O_2$	284	Octadecanoic acid
23	16.706	0.50	0.68	$C_7H_9FN_2O_2$	172	4-Fluoro-1-methyl-5-carboxylic acid, ethyl(ester)
24	16.932	0.90	1.21	$C_{12}H_{10}FN_5$	243	1H-Purin-6-amine, [(2-fluorophenyl) methyl]
25	17.031	0.99	1.15	$C_{19}H_{38}O_4$	330	Hexadecanoic acid, 2-hydroxy-1-(hydroxymethyl)ethyl ester
26	17.699	0.73	0.65	$C_{17}H_{29}NO_2$	279	12-cyano-15-hexadecanolide
27	19.022	0.48	0.72	$C_{11}H_{22}O$	170	Undecanal
28	21.874	1.54	1.01	$C_{21}H_{22}FEN_2O_5$	438	Iron, monocarbonyl-(1,3-butadiene-1,4-dicarbonic acid, diethyl ester) a,a'-dipyridyl
29	22.567	0.70	0.33	$C_{12}H_{15}N_3O_3$	249	2,4,6-Tris(Allyloxy)-S-triazine
30	23.736	0.93	0.56	$C_{12}H_{12}F_6O_2$	302	8,9,9,10,10,11-Hexafluoro-4,4-Dimethyl-3,5-dioxatetracyclo

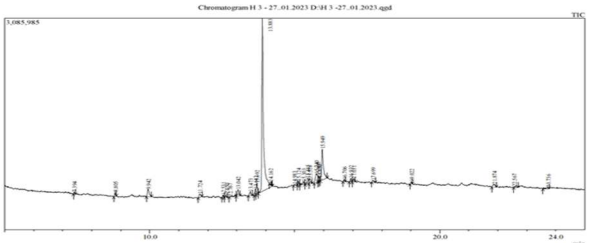

Figure 1: GC-MS chromatogram of *D. muricata* hydro-ethanolic leaf extract

HPLC Profiling of Phenolic and Flavonoid Compounds

HPLC analysis at 280 nm resolved 12 distinct peaks over the 25-min gradient run (Figure 2). All compound assignments (Table 3) are based on retention-time comparison with published chromatographic data. The largest peak (Peak 5, RT 6.457 min, 39.73%) was tentatively assigned to rutin. Ellagic acid (Peak 6, RT 9.657 min) accounted for 14.12% of the total peak area, and catechin (Peak 3, RT 3.112 min) for 11.49%. Peak 4 (RT 4.023 min, 20.61), indicating the presence of a major phenolic constituent. Based on its early elution profile, the compound is likely a low molecular weight polar phenolic, such as a hydroxybenzoic acid derivative. Additional tentatively identified constituents include kaempferol (Peak 1, 5.72%), quercetin (Peak 2, 3.53%), epicatechin (Peak 7, 1.52%), delphinidin-3-O-glucoside (Peak 8, 1.94%), delphinidin-3-O-rutinoside (Peak 9, 0.48%), catechol (Peak 10, 0.74%), quercetin-3-O-glucoside (Peak 12, 0.10%), and cyanidin-3-O-rutinoside (Peak 11, 0.03%).

Table 3: HPLC chromatographic profile of the hydro-ethanolic extract of *D. muricata*

Peak	RT (min)	Peak Area	Area %	Identified Compound
1	2.519	397240	5.723	Kaempferol
2	2.702	244829	3.527	Quercetin
3	3.112	797567	11.491	Catechin
4	4.023	1430411	20.609	Gallic acid
5	6.457	2757245	39.726	Rutin
6	9.657	980155	14.122	Ellagic acid
7	12.767	105411	1.519	Epicatechin
8	13.059	134541	1.938	Delphinidin-3-O-glucoside
9	15.183	33549	0.483	Delphinidin-3-O-retinoside
10	15.611	51056	0.736	Catechol
11	18.115	1907	0.027	Cyanidin-3-O-retinoside
12	29.485	6772	0.098	Quercetin-3-O-glucoside

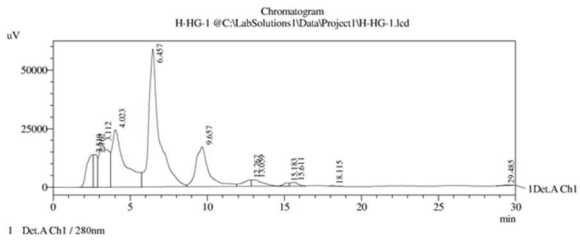

Figure 2: HPLC chromatogram as observed in the hydro-ethanolic extract of *D. muricata*

UV-Vis Spectroscopic Analysis

UV-Vis scanning over 200–1100 nm yielded five absorption bands (Table 4; Figure 3). The most intense absorption appeared at 202.6 nm (A = 4.000), consistent with electronic transitions associated with the conjugated double-bond system of aromatic rings at their fundamental excitation wavelength. A second well-defined peak at 250.1 nm (A = 1.571) falls within the characteristic Band-II absorption range of flavonoids (240–285 nm) and phenolic acids, and is consistent with the HPLC-tentative identification of rutin, kaempferol, quercetin, and catechin. Three low-intensity absorptions at 745.3, 843.9, and 988.2 nm (A ≈ 0.16–0.17) in the near-infrared region are attributed to C-H and O-H bond overtone vibrations; their low intensity and even spacing suggest an instrumental baseline feature or residual chlorophyll-derived absorbance rather than well-defined chromophoric transitions.

Table 4: UV-Vis absorption profile of the hydro-ethanolic extract of *D. muricata*

Peak	Wavelength (nm)	Absorbance (AU)
1	202.6	4.000
2	250.1	1.571
3	745.3	0.168
4	843.9	0.168
5	988.2	0.159

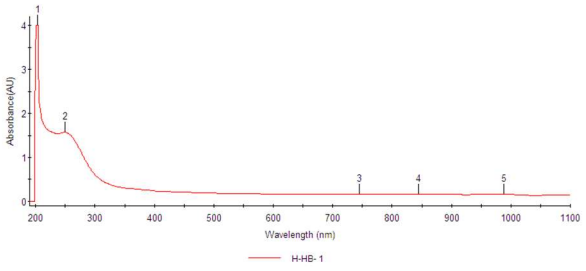

Figure 3: UV-Vis absorption spectrum of the *D. muricata* hydro-ethanolic extract

FTIR Functional Group Analysis

The spectral analysis of the extract using FTIR revealed 7 significant absorption bands in the range of 400-4000 cm^{-1} (Table 5; Figure 4). The wide absorption

at 3417.89 cm^{-1} is indicative of O-H stretching in phenolic hydroxyl groups and aliphatic alcohols and is broadened by intramolecular and intermolecular hydrogen bonds typical of polyphenolic assemblies [21]. The group of absorptions at 2977.92, 2929.10 and 2901.04 cm^{-1} are largely due to aliphatic C-H symmetric and asymmetric stretching vibrations (sp 3 C-H), and additional broad O-H contribution by carboxylic acids is likely to be overlapping. The 2127.12 cm^{-1} band is attributed to C≡C stretching of alkynes, which indicates the presence of polyacetylene-like metabolites, which is sometimes found in Amaranthaceae [22]. The absorption at 1645.27 cm^{-1} can be alkene C=C stretch (in line with phytol and 1-hexadecene) or conjugated C=C/C=O, in flavonoid A- and C-rings. The aromatic C-C ring at 1453.16, 1406.11 cm^{-1} corroborates the HPLC evidence of a polyphenolic structure. C-O stretching at 1065.69 and 1083.76 cm^{-1} are indicative of the ether and glycosidic C-O bonding of flavonoid O-glycosides like rutin and delphinidin-3-O-glucoside. The absorption at 879.43 cm^{-1} is attributable to out-of-plane C-H deformation of aromatic rings bearing substitution patterns consistent with flavonoid B-ring architectures.

Table 5: FTIR absorption bands and functional group assignments of *D. muricata* hydro-ethanolic extract

Frequency (cm^{-1})	Bond / Vibration	Functional Group
3417.89	O-H stretch, H-bonded	Alcohols, Phenols
2977.92, 2929.10, 2901.04	C-H / O-H stretch	Aliphatic chains; Carboxylic acids
2127.12	-C≡C- stretch	Alkynes
1645.27	-C=C- stretch	Alkenes
1453.16, 1406.11	C-C stretch (in-ring)	Aromatics
1065.69, 1083.76	C-O stretch	Alcohols, Ethers
879.43	C-H out-of-plane bend	Aromatics (substituted)

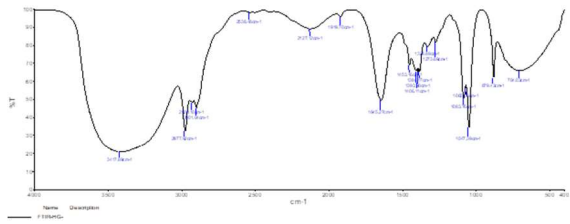

Figure 4: FTIR spectrum of *D. muricata* hydro-ethanolic extract

DISCUSSION

GC-MS Profile: Fatty Acid Dominance and Comparative Context

The presence of the n-hexadecanoic acid (palmitic acid, 57.08%) as the dominant hydrocarbon in the GC-MS profile of *D. muricata* hydro-ethanolic extract is another key finding that needs to be carefully contextualised. While palmitic acid is the most abundant saturated fatty acid in the plant kingdom and routinely reported as a major GC-MS constituent of polar plant extracts prepared from leafy material, its reported proportion in the present extract (>57%) is unusually high relative to comparable Amaranthaceae studies. Paranthaman et al. [19] also indicated palmitic acid as the most abundant in *Amaranthus caudatus* (~18 %), and research on *Amaranthus hybridus* reported palmitic acid as a major but not dominating GC-MS component (~21.99 %) [23]. The unusually large percentage in the present study can be explained by the lipophilic co-extraction of fatty acids linked to phospholipids in the membranes during hydro-ethanolic maceration, or could be because the extract was not de-fatted prior to GC-MS injection. The authors should comment on this and consider whether a de-fatting step prior to GC-MS analysis would reveal a more informative terpenoid and polyphenol volatile profile.

Pharmacologically, palmitic acid has been shown to exert antioxidant effects partly through membrane peroxidation resistance and partly through modulation of the Nrf2/HO-1 signalling axis [24]. Stearic acid (10.97%), the second most abundant GC-MS constituent, is increasingly recognised not as a mere structural lipid but as an active modulator of mitochondrial function and cellular signalling; Tao et al. [25] demonstrated its ability to inhibit NLRP3 inflammasome activation, offering a mechanistic basis for the anti-inflammatory ethnobotanical use of the plant. Phytol (1.51%), a diterpene alcohol that is released by chlorophyll during extraction, has also received pharmacological interest. Yu et al. [26] have shown phytol-induced apoptosis in colorectal cancer cell lines by accumulating ROS and disrupting mitochondrial membrane potential, which is consistent with the reported anticancer effects of *D. muricata* leaf extracts.

HPLC Polyphenolic Profile: Rutin, Ellagic Acid, and Antioxidant Significance

The HPLC analysis tentatively identifies rutin as the single largest polyphenolic constituent (39.73% peak area), a finding with substantive pharmacological implications. One of the most widely described bioactivity profiles in the literature is that of Rutin (quercetin-3-O-α-L-ramnopyranosyl-(1→6)- -glucopyranoside), a flavonoid O-glycoside. A 2022

meta-analysis of rutin's therapeutic potential by Azeem et al. [27] and Forouzanfar et al. [28] confirmed anti-inflammatory effects mediated through NF-κB pathway suppression, antidiabetic activity via α-glucosidase inhibition, and cardioprotective effects linked to reduced platelet aggregation. The high rutin content found here is consistent with prior HPTLC-fingerprint data from Usmani et al. [11], which implicated flavonoid glycosides as the dominant polyphenolic class in *D. muricata* methanolic extract and aligns with the exceptionally high total flavonoid content (193.18 mg QE/g) established in our preceding study [13].

Ellagic acid (14.12%) is a polyphenol tannin derivative of considerable chemopreventive interest. Zhao et al. demonstrated that ellagic acid suppressed HCT116 colorectal cancer cell proliferation at IC_{50} values below 100 µM through G0/G1-phase cell cycle arrest and thereby apoptosis [29]. Its presence at notable concentrations in *D. muricata* extract provides a mechanistic candidate for the antiproliferative activity documented against prostate and cervical cancer cell lines in prior work [8,9]. Catechin (11.49%) and its stereoisomer epicatechin (1.52%) are flavan-3-ols that donate hydrogen atoms to reactive radical species through their catechol B-ring and trihydroxy structure; the combination of catechin and epicatechin in the same extract, as observed here, is known to provide greater total antioxidant capacity than either compound alone owing to regenerative electron transfer between the two redox forms [30]. Kaempferol (5.72%) and quercetin (3.53%) eluted very close together (RT 2.519 and 2.702 min, respectively), reflecting their structural similarity (the sole difference being a hydroxyl substituent at the 3'-position of quercetin's B-ring). Both compounds have been extensively characterised as NF-κB, COX-2, and iNOS inhibitors [31].

The presence of anthocyanins, delphinidin-3-O-glucoside (1.94%) and cyanidin-3-O-retinoside (0.03%), is consistent with the qualitative Anthocyanin-positive result obtained for the hydro-ethanolic extract in our parent study [13]. Anthocyanins contribute to visual pigmentation and act as singlet oxygen quenchers and transition metal chelators. Their relatively minor abundance (combined <2%) suggests that flavonol glycosides and hydrolysable tannins (rutin and ellagic acid) are the primary antioxidant contributors in this extract, as would be expected from a leafy extract where anthocyanins typically accumulate in response to environmental stress rather than constitutively [32].

UV-Vis and FTIR: Spectroscopic Validation of Phytochemical Classes

The UV-Vis spectrum reinforces the polyphenolic composition inferred from HPLC. The absorption at 202.6 nm corresponds to the primary electron transition of the benzene ring, a feature common to all aromatic compounds and present in every flavonoid and phenolic acid identified. The 250.1 nm band aligns with the characteristic Band-II absorption (cinnamoyl system) of flavones, flavonols, and their glycosides, which typically absorb between 240 and 270 nm [33]. Notably absent are the strong Band-I absorptions (340–390 nm for flavonols; 300–330 nm for flavones) that would be expected if the flavonoid chromophores were present at high enough concentrations for individual electronic transitions to be resolved in the mixture spectrum. This may reflect the spectroscopic averaging effect of the highly complex extract matrix, or it may indicate that the extract was too concentrated in the 300–400 nm region, causing detector saturation. A dilution series in future work would clarify this. The near-infrared absorptions at 745–988 nm are of low diagnostic utility without a reference spectrum; their even spacing and uniformly low absorbance (~0.17) is more consistent with a grating order artefact or a flat near-IR scattering baseline than with distinct molecular transitions, and the authors should exercise caution in assigning these to specific structural features.

FTIR spectrum also offers complementary functional-group-level data in agreement with the molecular inventory determined by GC-MS and HPLC. The O-H breadth at 3417 cm^{-1} is predominantly of the phenolic hydroxyl groups and the breadth of the OH - 3417 cm^{-1} breadth - probably comprising 3200-3600 cm^{-1} - reflects the large intermolecular hydrogen bonding network of the polyphenolic matrix, which is well-documented in FTIR literature in flavonoid-rich plant extracts [21]. The aliphatic C-H stretches at 2901–2978 cm^{-1} are fully consistent with the long-chain methylene skeleton of palmitic and stearic acids. The 1645 cm^{-1} band itself is multivalent: in flavonoid chromophores, the C4=O carbonyl of the γ-pyrone ring typically appears near 1640–1680 cm^{-1} depending on hydroxylation pattern, and the conjugated C=C of the chromone backbone absorbs in a similar region, making this band a useful but non-specific marker [34]. C-O stretch of 1065 and 1083 cm^{-1} is indicative of aryl ether and O-glycosidic linkages that confirm the nature of the dominant flavonoid O-glycoside (rutin) obtained by HPLC.

Cross-Platform Integration and Bioactivity Rationalisation

Combined, the four sets of analysis narrow down to a logical phytochemical story of the *D. muricata* leaf hydro-ethanolic extract. The high total phenolic content documented in the parent study (246.82 mg GAE/g) is now given molecular identity through the HPLC-tentative identification of rutin, ellagic acid, catechin, kaempferol, and quercetin, all well-characterised, potent Folin-Ciocalteu-reactive phenolics. The high total flavonoid content (193.18 mg QE/g by $AlCl_3$ colorimetry) is accounted for primarily by the rutin

peak (39.73%), consistent with the known hyperchromic response of rutin in the aluminium chloride assay. The saponin content (134.76 mg SE/g) is high, but none of the constituents found in the GC-MS or HPLC analyses would explain such a high saponin content. Saponins are highly polar amphiphilic glycosides that are not easily detected by the RP-HPLC conditions or GC-MS technique used in this study. Similarly, the steroid content (117.66 mg CE/g by Liebermann-Burchard assay) reflects phytosterols and triterpene glycosides that are non-volatile and chromatographically inaccessible under the current GC-MS conditions.

From a mechanistic antioxidant perspective, rutin and quercetin scavenge free radicals via the ortho-dihydroxy (catechol) moiety on their B-rings, which acts as a hydrogen-atom donor to peroxyl and hydroxyl radicals; the resulting semiquinone radical is stabilised by resonance delocalisation across the entire flavone skeleton. This mechanism is corroborated by the FTIR evidence of strong O-H absorption (3417 cm^{-1}) and C-O stretching (~1065 cm^{-1}), and the UV-Vis confirmation of extended conjugation (250.1 nm). Ellagic acid acts in an alternative but complementary way: its four hydroxyl groups on the biphenyl scaffold have the metal chelation properties against redox-active iron and copper ions, thus inhibiting Fenton-type hydroxyl radical formation. Although the palmitic acid fraction is less reactive in the classical DPPH/FRAP assays, it might provide antioxidant protection at the membrane level through competitive incorporation into phospholipid bilayers and, therefore, decrease the share of oxidation-prone polyunsaturated fatty acids [24].

CONCLUSION

This study provides the first integrated multi-analytical characterisation of the bioactive phytoconstituents in the hydro-ethanolic leaf extract of *Digera muricata*. GC-MS analysis establishes a fatty-acid-rich volatile profile dominated by n-hexadecanoic acid (57.08%) and octadecanoic acid (10.97%), with pharmacologically significant terpenoids, phytol and tetradecanoic acid, present as minor constituents. HPLC profiling indicates a tentative polar fraction, a flavonoid and phenolic acid-rich fraction with rutin (39.73%), ellagic acid (14.12%), and catechin (11.49%) as the major constituents. UV-Vis spectroscopy confirms the presence of aromatic chromophores and flavonoid Band-II absorbers, consistent with the HPLC profile. FTIR spectroscopy visualizes the functional group distribution of the extract, which supports the existence of phenolic O-H, aliphatic C-H chains, alkene C=C and glycosidic C-O bonds. Collectively, these data give a rationalisation of the antioxidant, anti-inflammatory, and anticancer activities of this plant at the molecular level and rutin, ellagic acid and phytol as the most promising molecular targets to be isolated, purified and their bioactivity validated *in vitro/in vivo.*

ACKNOWLEDGEMENTS

The authors would like to thank Department of Biochemistry, VISTAS for providing the necessary facilities for our research work.

AUTHORS CONTRIBUTIONS

All the authors have contributed equally to this article

CONFLICT OF INTEREST

There are no conflicts of interest.

REFERENCES

1. Karuppannan SK, Dowlath MJH, Mohamed Khalith SB, Darul Raiyaan GI, Subramanian S, Arunachalam KD. Phytochemical and antibacterial activity of *Cardiospermum halicacabum* against wound pathogens. Pharmacogn J. 2020;12:1303–1310.
2. Newman DJ, Cragg GM. Natural products as sources of new drugs over the nearly four decades from 1981 to 2019. J Nat Prod. 2020;83:770–803.
3. Ankul SS, Gowri K, Chitra V. A review on phytochemical constituents and pharmacological activities of the plant *Aerva lanata*. Res J Pharm Technol. 2020;13:1580–1586.
4. Ndukwe GI, Clark PD, Jack IR. In vitro antioxidant and antimicrobial potentials of three extracts of *Amaranthus hybridus* leaf and their phytochemicals. Eur Chem Bull. 2020;9:164–173.
5. Sharma P, Saini S, Hasanpuri P, Kataria N, Kumar V, Singh P, Sharma A. Recent progress in ethnobotany, phytochemistry, pharmacology, and toxicology of wild plants of family Amaranthaceae: An updated review. Beni-Suef Univ J Basic Appl Sci. 2025;14:87.
6. Parrotta JA. Healing plants of peninsular India. 2001.
7. Khan MR, Rizvi W, Khan GN, Khan RA, Shaheen S. Carbon tetrachloride-induced nephrotoxicity in rats: Protective role of *Digera muricata*. J Ethnopharmacol. 2009;122:91–99.
8. Usmani S, Hussain A, Farooqui AHA, Arshad M, Siddiqui S, Ahmad M, Wahab S. Anti-proliferative activity of crude extract and fractions of *Digera muricata* on HeLa and A549 cell lines. Pharmacogn J. 2014;6.
9. Vidyashri S, Elumalai P, Raghunandhakumar S, Lakshmi T, Roy A. Anticancer effect of *Digera muricata* leaf extract against prostate cancer cell lines. J Pharm Anal. 2021;33:431–438.
10. Mathad P, Mety SS. Phytochemical and antimicrobial activity of *Digera muricata*. J Chem. 2010;7:275–280.
11. Usmani S, Hussain A, Farooqui AHA, Khatoon S. HPTLC fingerprinting and antioxidant potential of methanolic extract of *Digera muricata*. J Chem Pharm Res. 2015;7:661–665.

12. Shah R, Shah SA, Shah S, Faisal S, Ullah F. Green synthesis and antibacterial activity of gold nanoparticles of *Digera muricata*. Indian J Pharm Sci. 2020;82:374–378.
13. T S, V R, A P, R V. Qualitative and quantitative phytochemical profiling of *Digera muricata* leaves. J Adv Zool. 2023;44:833–838.
14. Cunha-Chiamolera TPL, Chileh-Chelh T, Urrestarazu M, Ezzaitouni M, López-Ruiz R, Gallón-Bedoya M, Rincón-Cervera M, Guil-Guerrero JL. Crop productivity, phytochemicals, and bioactivities of *Amaranthus viridis*. Agronomy. 2024;14:2038.
15. Arshad HM, Ahmad FUD, Lodhi AH. Methanolic extract of *Aerva javanica* prevents LPS-induced depressive-like behavior in mice. Drug Des Devel Ther. 2022;16:4179–4204.
16. Mossa ATH, Nawwar GAM. Free radical scavenging and antiacetylcholinesterase activities of *Origanum majorana* essential oil. Hum Exp Toxicol. 2011;30:1501–1513.
17. Murkovic M. Phenolic compounds: Occurrence, classes, and analysis. Encycl Food Health. 2016;346–351.
18. Dowlath M, Karuppannan SK, Darul R, Mohamed K, Subramanian S, Arunachalam KD. Effect of solvents on phytochemical composition and antioxidant activity of *Cardiospermum halicacabum* extracts. Pharmacogn J. 2020;12:1241–1251.
19. Paranthaman R, Praveen KP, Kumaravel S. GC-MS analysis of phytochemicals and flavonoids in *Amaranthus caudatus*. J Anal Bioanal Tech. 2012;3.
20. Seal T. Quantitative HPLC analysis of phenolic acids, flavonoids and ascorbic acid in wild edible leaves. J Appl Pharm Sci. 2016;6:157–166.
21. Silverstein RM, Bassler GC. Spectrometric identification of organic compounds. J Chem Educ. 1962;39:546.
22. Christensen LP, Brandt K. Bioactive polyacetylenes in Apiaceae plants: Occurrence, bioactivity and analysis. J Pharm Biomed Anal. 2006;41:683–693.
23. Dania OE, Dokunmu TM, Iweala EEJ. Comparison of bioactive components in *Corchorus olitorius* and *Amaranthus hybridus*. Trop J Nat Prod Res. 2024;8:8150–8154.
24. Shi Y, Sun Y, Sun X, Zhao H, Yao M, Hou L, Jiang L. Up-regulation of HO-1 by Nrf2 activation protects against palmitic acid-induced ROS increase. Nutr Res. 2018;52:80–86.
25. Tao Y, Wang N, Qiu T, Sun X. Role of autophagy and NLRP3 inflammasome in liver fibrosis. Biomed Res Int. 2020;2020:7269150.
26. Yu J, Jin F, Tang Y, Huang Y. In vitro anticancer activity of phytol on A549 cells. Integr Cancer Ther. 2025;24:15347354251344592.
27. Azeem M, Niazi S, Fayyaz F, Zahoor A, Zehra T, Fatima M, Abid HMU. Overview of pharmacological effects of rutin. Curr Pharm Res. 2024;2:119–155.
28. Forouzanfar F, Sahranavard T, Tsatsakis A, Iranshahi M, Rezaee R. Rutin: A pain-relieving flavonoid. Inflammopharmacology. 2025;33:1289–1301.
29. Zhao J, Li G, Ren Y, Zhang Z, Chen H, Zhang H, Zhao X, Li W, Jia Y, Guan X, Liu M. Ellagic acid inhibits colon cancer cells via lncRNA regulation. Anticancer Drugs. 2023;34:1112–1121.
30. Perron NR, Brumaghim JL. Antioxidant mechanisms of polyphenols related to iron binding. Cell Biochem Biophys. 2009;53:75–100.
31. Formica JV, Regelson W. Review of the biology of quercetin and related bioflavonoids. Food Chem Toxicol. 1995;33:1061–1080.
32. Castañeda-Ovando A, Pacheco-Hernández ML, Páez-Hernández ME, Rodríguez JA, Galán-Vidal CA. Chemical studies of anthocyanins: A review. Food Chem. 2009;113:859–871.
33. Harborne JB, Williams CA. Advances in flavonoid research since 1992. Phytochemistry. 2000;55:481–504.
34. Coates J. Interpretation of infrared spectra: A practical approach. Encycl Anal Chem. 2000.